EARTHQUAKE ENGINEERING AND STRUCTURAL DYNAMICS
Earthquake Engng. Struct. Dyn. **28**, 691–706 (1999)

EFFECTS OF TORSION FACTORS ON SIMPLE NON-LINEAR SYSTEMS USING FULLY-BIDIRECTIONAL ANALYSES

J. DE-LA-COLINA*
Facultad de Ingeniería, Universidad Autónoma del Estado de México, Toluca Edo. de México, México

SUMMARY

An ensemble of earthquake records is used to carry out non-linear analyses of simple torsionally unbalanced systems considering both resisting elements and earthquake components along two perpendicular directions. These fully bidirectional analyses are focused to study the effect of the following factors: (i) seismic-force reduction factor; (ii) factors α and δ used to compute the design eccentricity; (iii) initial lateral period; and (iv) initial stiffness eccentricity. Results indicate that the amplification factor α can be specified as a function of the force reduction factor, the lateral uncoupled period, and the stiffness eccentricity. It is concluded that the coefficient δ depends on the lateral period, the stiffness eccentricity, and the geometrical eccentricity. It was observed that negative shears caused by torsion should be neglected in the design of the stiff element, particularly in the case of systems with large stiffness eccentricity. Results suggest that additional studies should be performed to verify the assumed (partial) equivalence between unidirectional (resisting elements and earthquake components along one direction only) and fully bidirectional analyses to study building torsion problems. Copyright © 1999 John Wiley & Sons, Ltd.

KEY WORDS: seismic response; torsion; buildings; seismic design; bidirectional analysis

INTRODUCTION

The behaviour of torsionally unbalanced non-linear systems has been studied extensively in the last years.[1–3] In these studies the structural system has been limited to one-storey models where the main variables evaluated are: (i) the design code coefficients, (ii) the lateral uncoupled period of vibration, (iii) the stiffness eccentricity, and (iv) the seismic-force reduction factor usually denoted by R. Several building codes[4–6] specify design eccentricities e_{d} as a function of the coefficients α, δ, and β as follows:

$$e_{\mathrm{d}1} = \alpha e_{\mathrm{s}} + \beta b = \alpha e_{\mathrm{s}} + e_{\mathrm{a}} \tag{1a}$$

$$e_{\mathrm{d}2} = \delta e_{\mathrm{s}} - \beta b = \delta e_{\mathrm{s}} - e_{\mathrm{a}} \tag{1b}$$

* Correspondence to: J. De-la-Colina, Facultad de Ingeniería, Universidad Autónoma del Estado de México, Apartado Postal 2-94, Toluca Edo. de México, México. E-mail: jcolina@coatepec-uaemex.mx

CCC 0098–8847/99/070691–16$17·50

Received 3 February 1998
Revised 30 June 1998 and 1 October 1998

where e_s is the stiffness eccentricity (distance between the centre of mass CM and the centre of rigidity CR), β is a coefficient to estimate the accidental eccentricity e_a and b is the slab dimension in the direction of the eccentricity. Depending upon the design code, the factor α takes the value of 1·0 or 1·5, while the factor δ takes the value of 0.0, 0.5, or 1·0. Factor α is intended to compensate the difference between dynamic and static analyses (dynamic amplification). Factor δ specifies the portion of the torsion-induced negative shear that can be reduced for the design of the stiff-side resisting elements. The accidental-eccentricity factor β, associated with the uncertainty on the location of CM and CR, usually takes the value of 0.05 or 0.10.

One of the first studies carried out to evaluate the effect of the force reduction factor R was conducted by Goel and Chopra.[1] Their study used a system with resisting elements oriented in both directions but considering the ground motion in one direction only (*partially bidirectional analysis*). They concluded that large values of R could lead to the use of small values of α. A subsequent study by Chandler and Duan,[3] based on systems with elements oriented along one direction only (*unidirectional analysis*), concluded that the force reduction factor R influences the stiff-side resisting element significantly but it has little effect on the flexible-side element. The latter conclusion seems to discard the relationship between α and R suggested by Goel and Chopra because α mainly affects flexible-side elements.

Most of the studies on building torsion, however, have considered systems with resisting elements or earthquake excitations oriented in one direction only (*unidirectional or partially bidirectional analysis*). The study by Wong and Tso,[7] which used both resisting elements and earthquake components along two directions (*fully bidirectional analysis*), was limited to assess the effect of reducing the torsion-induced shears in systems designed according with a recent edition of the *Uniform Building Code*.[6] Although Correnza *et al.*[8] concluded that unidirectional analyses provide good estimates of fully bidirectional analyses (except for flexible-edge elements in short-period systems), the scope of some variables they considered was limited (e.g. force reduction factor, stiffness eccentricity, etc.). This leaves the cited equivalence open to questions and motivates recent studies[9,10] to use fully bidirectional analyses.

In this study, fully bidirectional analyses are carried out to evaluate the effect of the following factors on the response of simple non-linear torsionally unbalanced systems: (i) the force reduction factor R, (ii) the design factors α and δ, (iii) the uncoupled lateral period T, and (iv) the stiffness eccentricity e_s. Possible relationship of factors α and δ to R, T or e_s is also explored. The equivalence between uni- and fully bidirectional analyses is briefly studied also. The coefficient β, which is required to compute the design eccentricity, is not assessed in this paper because the locations of both CM and CR are completely defined in the modelling. The issue of including an accidental eccentricity in this type of studies has been discussed widely;[3] however, no conclusive answers have been obtained.

STRUCTURAL MODEL

The structural model used in this study is similar to that used by Wong and Tso[7] and it consists of a rigid rectangular slab with mass m and size a by $b = 2a$ (Figure 1). The distribution of mass is similar to that considered by Tso and Zhu[2] where part of m is uniformly distributed on the area and the rest is located on one edge of the slab short side. The slab is supported by six resisting elements: three oriented in the X direction and three in the Y direction. These elements provide resistance in their planes only. The pre-yield stiffness of each element is selected so that the centre

of rigidity CR is initially located at a distance $e_g = \eta b$ to the left of the geometrical centre of the slab along the X-axis. Thus, the parameter η defines the position of CR but it does not define the unbalance caused by torsion. The stiffness eccentricity e_s is defined by the distance from the centre of rigidity CR to the centre of mass CM, $e_s = eb$. Systems with $e_s = 0$ are torsionally balanced (TB) and those with $e_s > 0{\cdot}0$ are torsionally unbalanced (TU).[2] The X-axis is a symmetry axis and CM is located along this axis. The resisting force of elements 1 and 3 is assumed to act at a distance $b/2$ of the central element (element 2). The element 5 is located along the X-axis and the elements 4 and 6 are located at a distance $d/2$ below and above the X-axis, respectively.

The total stiffness along both directions is assumed to be the same ($K_X = K_Y = K$) and, therefore, the uncoupled lateral periods are the same also: $T_X = T_Y = T$. As for the resisting elements, their initial stiffnesses were selected as follows. The stiffness of element 2, k_2, was assumed to be equal to the stiffness of element 3, k_3. Therefore, for a given value of η, the stiffness of element 3 is given by $k_3 = 2K_Y(0{\cdot}5 - \eta)/3$. Moreover, for a given period and mass, which define the total stiffness, $k_1 = K_Y - k_2 - k_3$. It is assumed that in the X-direction $k_5 = k_4/2 = k_6/2$. This implies that $k_4 = k_6 = 2K_X/5$ and that $k_5 = K_X/5$.

The investigation associated with this paper studied the response of these systems with the following values: $\eta = 0{\cdot}0$, $0{\cdot}2$, and $0{\cdot}4$; $e = 0{\cdot}0$, $0{\cdot}05$, and $0{\cdot}20$; $d/a = 0{\cdot}0, 0{\cdot}1, 0{\cdot}2, \ldots, 1{\cdot}0$; $T = 0{\cdot}5$ s, $1{\cdot}0$ s, and $1{\cdot}5$ s.; $R = 1$, 3, and 6; $\alpha = 1{\cdot}0$ and $1{\cdot}5$; and $\delta = 0{\cdot}0$, $0{\cdot}5$, and $1{\cdot}0$. The values of the dimensionless eccentricities η and e were selected to cover a wide range of eccentricity posibilities and to identify behaviour trends. However, it is important to notice that the combination of some values of these eccentricities can be unrealistic, e.g. the combination of $\eta = 0{\cdot}4$ and $e = 0{\cdot}05$.

In similar torsion studies[2,3] the response parameters have been presented in terms of the quantity $\rho_k = (K_\theta/K)^{1/2}/b$, where K_θ is the torsional stiffness of the system. However, in this study the normalized distance between X-direction resisting elements d/a is selected by the following reasons. First, both terms ρ_k and d/a increase with growing values of the torsional stiffness (Table I lists the equivalences between d/a and ρ_k for three values of η used). Second, values of ρ_k vary with η while those of d/a do not, which avoids to use several ranges of ρ_k. Third, the value of ρ_k is related to the torsional stiffness provided by all elements, while d/a is related to the torsional stiffness provided by transverse elements only. The use of d/a allows to study the participation of transverse elements (elements 4 and 6 in Figure 1) in the torsional response of the system. The value $d/a = 1{\cdot}0$ corresponds to the largest torsional stiffness of the system and the value $d/a = 0{\cdot}0$ corresponds to the uncoupling of the transverse elements.

Table I. Values of ρ_k in terms of d/a and η

Dimensionless distance d/a	ρ_k		
	$\eta = 0{\cdot}0$	$\eta = 0{\cdot}2$	$\eta = 0{\cdot}4$
0·0	0·408	0·400	0·271
0·2	0·411	0·403	0·275
0·4	0·418	0·410	0·285
0·6	0·430	0·422	0·302
0·8	0·446	0·438	0·325
1·0	0·465	0·458	0·351

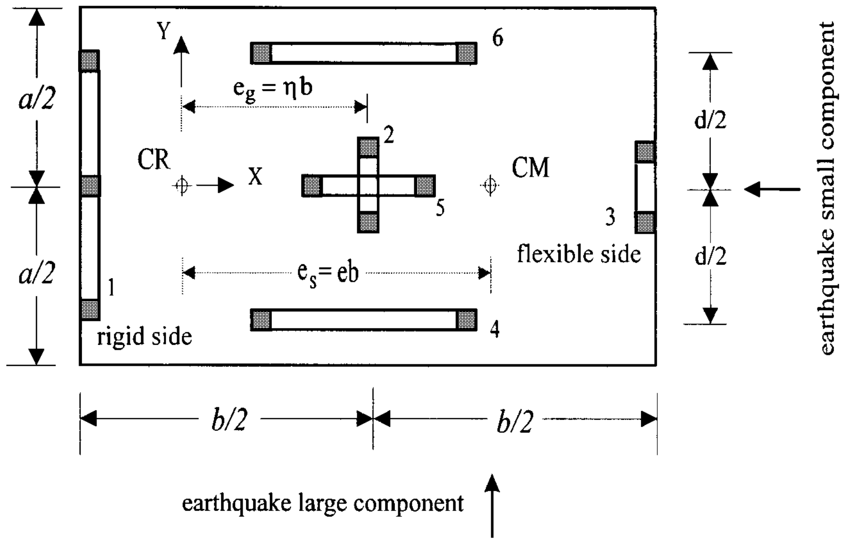

Figure 1. Torsionally unbalanced system

The resisting elements are assumed to have a non-linear response defined by the Clough[11]–Otani[12] model, which is typical of reinforced concrete elements in flexure. Although the choice of the model is not very significant, this stiffness-degrading model was selected because (i) it is more realistic for reinforced concrete elements (most of the buildings damaged by torsion during the 1985 Mexico earthquake were made of reinforced concrete) and (ii) stiffness-degrading models lead to smoother response spectra than bilinear models[13] (this facilitates the interpretation of results by reducing peaks in the response curves). The post-yield stiffness of each element is considered to be equal to 10 per cent of the corresponding initial stiffness. In this hysteretic model, the unloading stiffness is defined by both the maximum displacement attained (relative to the yield displacement) and the exponent α_c (Figure 2). For all the resisting elements considered here $\alpha_c = 0{\cdot}4$.

Another important characteristic of the designed systems is the strength eccentricity, e_p (measured with respect to the initial position of CR). For the systems considered here, most of the values of e_p are smaller than the values of e_s, which is typical of code-designed systems (see Figure 3). To be consistent with the elastic design spectra described below a Rayleigh damping of 5 per cent was included in all systems using the first two modes of vibration of the linear behaviour.

GROUND MOTIONS AND DESIGN SPECTRA

An ensemble of ten pairs of earthquake records (Table II) were used to compute the response of the systems. The records were selected to be consistent with the Newmark–Hall[14] design spectra. The ground motion was assumed to be bidirectional with the largest component parallel to the Y-axis. For each pair of motions, the record with the largest peak ground acceleration was

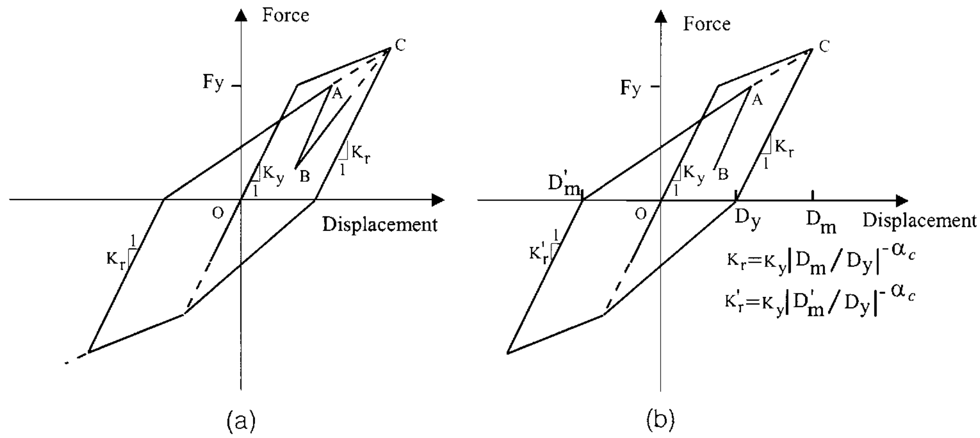

Figure 2. Clough–Otani hysteretic model: (a) original Clough model; (b) modified Clough–Otani model

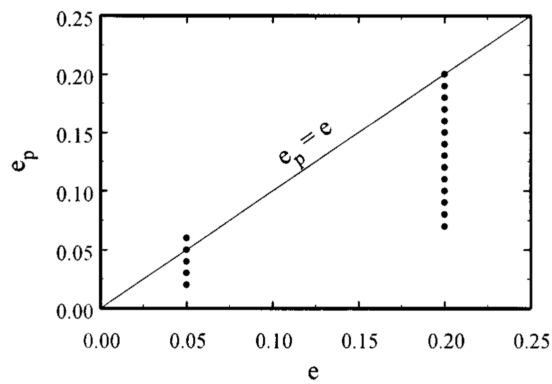

Figure 3. Positions of the strength centre e_p in terms of e

normalized to $1g$ using a scale factor. Each perpendicular component, to act in X-direction, was scaled with the same factor of this pair. For design, the lateral forces along X and Y directions were computed as follows:

$$F_x = ma_x/R, \qquad F_y = ma_y/R \tag{2}$$

where a_x and a_y are the design spectral accelerations. In the Y-direction the spectral acceleration was obtained of a 5 per cent-damped Newmark–Hall spectrum normalized to a peak ground acceleration of $1g$. In the X-direction the spectral acceleration was obtained of a similar spectrum but normalized to the mean value of the individually scaled peak accelerations of the perpendicular earthquake components ($0{\cdot}64g$). The mean acceleration response spectra as well as the design spectra are shown in Figure 4.

The lateral forces lead to the definition of the yield force of each resisting element using equations (3) and (4). These equations, however, are based on linear-elastic properties and assign

Table II. Earthquake ground motions

Earthquake	Station	Components	Used duration (s)	Max. ground accelerations
Imperial Valley, May/18/1940	El Centro	S90W, S00E	20	0·21g, 0·35g
Kern County, July/21/1952	Santa Barbara	N42E, S48E	20	0·09g, 0·13g
México (Mich.), Sept/19/1985	La Union	EW, NS	60	0·15g, 0·17g
México (Mich.), Sept/19/1985	Papanoa	EW, NS	60	0·12g, 0·17g
San Salvador, Oct/10/1986	Nat. Inst. of Geo.	NS, EW	20	0·40g, 0·53g
San Salvador, Oct/10/1986	Geo. Res. Center	NS, EW	8	0·42g, 0·69g
Loma Prieta, Oct/17/1989	Corralitos	EW,NS	20	0·48g, 0·63g
Loma Prieta, Oct/17/1989	Presidio	NS, EW	20	0·10g, 0·20g
Northridge, Jan/17/1994	Sylmar/Hospital Park.	EW, NS	20	0·60g, 0·84g
Northridge, Jan/17/1994	S. Monica/City Hall G.	NS, EW	20	0·37g, 0·88g

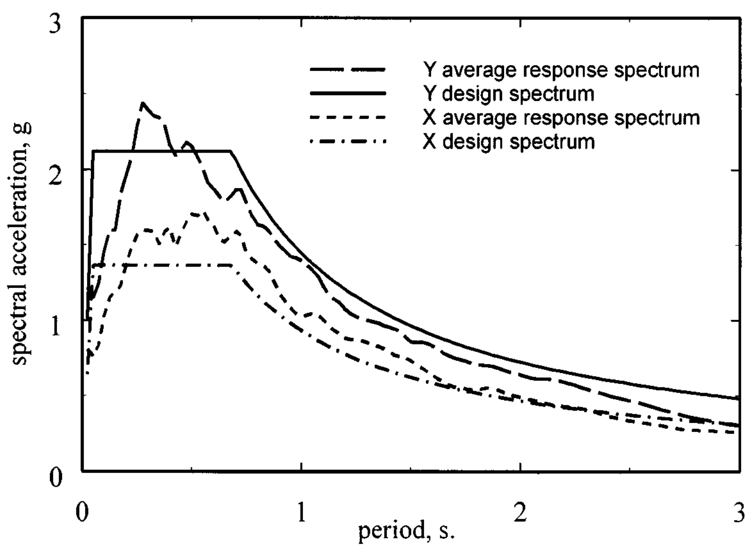

Figure 4. Mean-acceleration response and design spectra

strength in proportion of element stiffnesses. The use of these equations also assumes that yield displacement of each element is achieved simultaneously. However, this may be not true for wall structures where yield displacement is not proportional to stiffness but to wall length as shown by Paulay:[15,16]

$$F_{y1} = \frac{ma_y}{R}\left[\frac{k_1}{K_y} + \delta e_s \frac{k_1 x_1}{K_\theta}\right], \quad F_{y2} = \frac{ma_y}{R}\left[\frac{k_2}{K_y} + \alpha e_s \frac{k_2 x_2}{K_\theta}\right], \quad F_{y3} = \frac{ma_y}{R}\left[\frac{k_3}{K_y} + \alpha e_s \frac{k_3 x_3}{K_\theta}\right] \tag{3}$$

$$F_{y4} = \frac{m}{R}\left[a_x \frac{k_4}{K_x} + a_y \alpha e_s \frac{k_4(-y_4)}{K_\theta}\right], \quad F_{y5} = \frac{ma_x k_5}{RK_x}, \quad F_{y6} = \frac{m}{R}\left[a_x \frac{k_6}{K_x} + a_y \alpha e_s \frac{k_6 y_6}{K_\theta}\right] \tag{4}$$

COMPUTED RESPONSE

The inelastic response is computed numerically solving the equations of motion with the Newmark β (constant acceleration) method. The main response parameter of interest selected for this paper is the ductility demand of both the rigid-side element (element 1) and the flexible-side element (element 3). The ductility demands are normalized with respect to the corresponding values of the torsionally balanced system ($e = 0{\cdot}0$). These normalized quantities reflect the additional ductility caused by torsion in the TU systems as compared with that in TB systems. The slab rotation was also computed to analyze its variation with R. The mean value of both the normalized quantities and the slab rotations, over the ensemble of records, are used here in order to have smooth response curves.

Although the main parameter selected is the normalized displacement ductility demand, it is important to bear in mind that this parameter should be interpreted along with displacements in order to obtain general conclusions. For instance, if computed ductility demands for the flexible-side element of TU systems result of the same order than those of TB systems and this response parameter is considered only, the conclusion could be that the flexible element is not

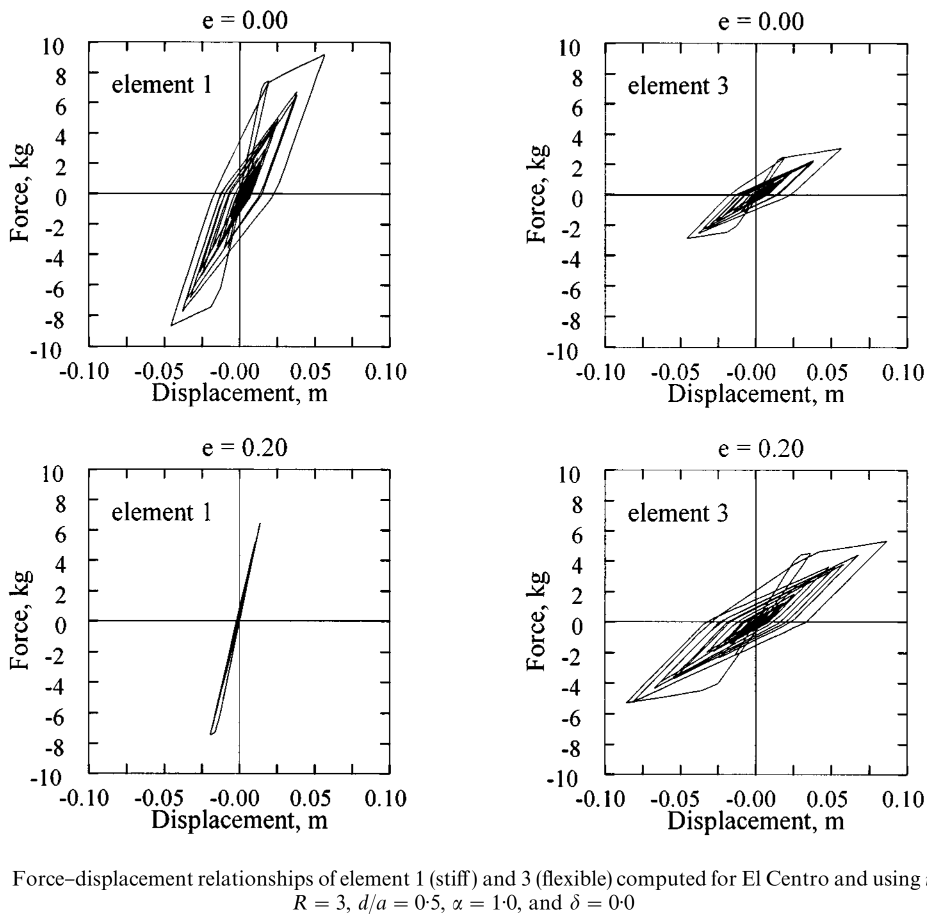

Figure 5. Force–displacement relationships of element 1 (stiff) and 3 (flexible) computed for El Centro and using $\eta = 0{\cdot}20$, $R = 3$, $d/a = 0{\cdot}5$, $\alpha = 1{\cdot}0$, and $\delta = 0{\cdot}0$

critical during torsion. However, if it is noticed that the displacements of this element grows appreciably also, the conclusion could be that the hysteretic energy dissipated by the element increases with torsion. In the latter case the flexible element would be critical, as noted by Goel.[9] In the present study, the same observation obtained by Goel,[9] in terms of hysteretic energy, is obtained, i.e. torsion causes both an increase of hysteretic work for the flexible element and a reduction for the stiff one (Figure 5). At this point it is interesting to note that, based on normalized ductility demands, Chandler and Duan[3] concluded that the stiff element is more critical than the flexible one.

Although the results presented below help to get some insight in the behaviour of multistorey buildings with torsion, it is important to bear in mind that additional studies should be carried out to study the non-linear behaviour of multistorey structures. This is particularly important for structural configurations wherein centers of mass (and/or rigidity) are not vertically aligned.

Effect of the force-reduction factor R

Figure 6 shows the normalized ductility demand of elements 1 and 3 in terms of the normalized distance between X-axis-parallel exterior elements d/a. Left-side graphs correspond to the stiff element (element 1) and those on the right side correspond to the flexible element (element 3). The four upper graphs in the same figure were obtained using $\alpha = 1{\cdot}0$ while the four lower ones were obtained with $\alpha = 1{\cdot}5$. Two values of the initial stiffness eccentricity are identified in each group ($e = 0{\cdot}05$ for first and third rows and $e = 0{\cdot}20$ for second and fourth rows). All cases in this figure were computed using $\eta = 0{\cdot}4$, $\delta = 0{\cdot}0$ and $T = 0{\cdot}5$ s. Computed normalized ductility demands for $\eta = 0{\cdot}0$ (not shown here) indicate the the effect of R is smaller for systems with $\eta = 0{\cdot}0$ than for systems with $\eta = 0{\cdot}4$, although the trends are the same. For each graph of Figure 6, plots are presented for three values of the reduction factor ($R = 1$, 3, and 6). Graphs on the left side indicate that the normalized ductility demand of the stiff-side element μ_{n1} does not change significantly with R in the range of d/a ($0{\cdot}271 \leq \rho_k \leq 0{\cdot}351$). For these rigid-element graphs the value of μ_{n1} is almost entirely smaller than 1·0; which means that the ductility demand of rigid elements of TU systems is smaller than the corresponding demand of TB systems (see also left-side graphs in Figure 5). On the other hand, right-side graphs indicate that the ductility demand of the flexible element μ_{n3} decreases with increasing values of the force reduction factor. This result is congruent with that obtained by Goel and Chopra,[1] who suggested a reduction of α with R. It is interesting to observe that the results presented here do not coincide with those obtained by Chandler and Duan[3] based on *unidirectional analyses*. They concluded that, for $T = 2{\cdot}5$ s and $e = 0{\cdot}3$, μ_{n1} is very significantly influenced by R. Moreover, they observed that R has little effect on μ_{n3}.

The slab rotation has been another interesing issue analysed by several researchers.[1,3] Most of them conclude that rotation is reduced with increasing values of the reduction factor R. Results of this work are shown in Figure 7, where slab rotation is plotted against the ratio d/a. Graphs in this figure are organized as follows. Those on the left side correspond to systems with $\eta = 0{\cdot}0$ ($0{\cdot}408 \leq \rho_k \leq 0{\cdot}465$) while those on the right side correspond to systems with $\eta = 0{\cdot}4$ ($0{\cdot}271 \leq \rho_k \leq 0{\cdot}351$). The four upper graphs correspond to systems designed with $\alpha = 1{\cdot}0$ while the four lower ones correspond to systems designed with $\alpha = 1{\cdot}5$. Two values of stiffness eccentricity are considered for each group also. Results show that slab rotation decreases with increasing values of the reduction factor R. The amount of reduction is larger for systems with $\eta = 0{\cdot}4$ than for systems with $\eta = 0{\cdot}0$ because the considered range of variation of ρ_k is larger in the first case than

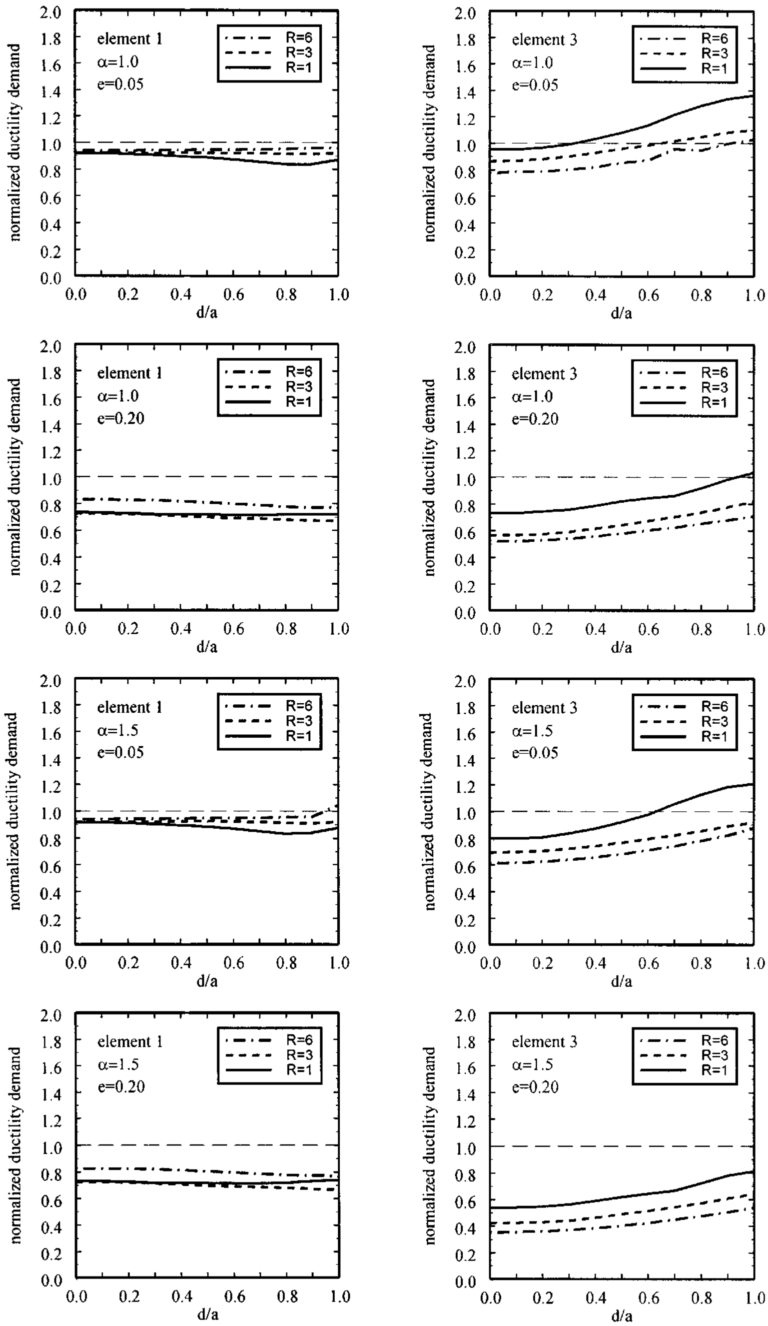

Figure 6. Normalized ductility demands of elements 1 and 3 for $\eta = 0{\cdot}4$, $\delta = 0{\cdot}0$, and $T = 0{\cdot}5$ s

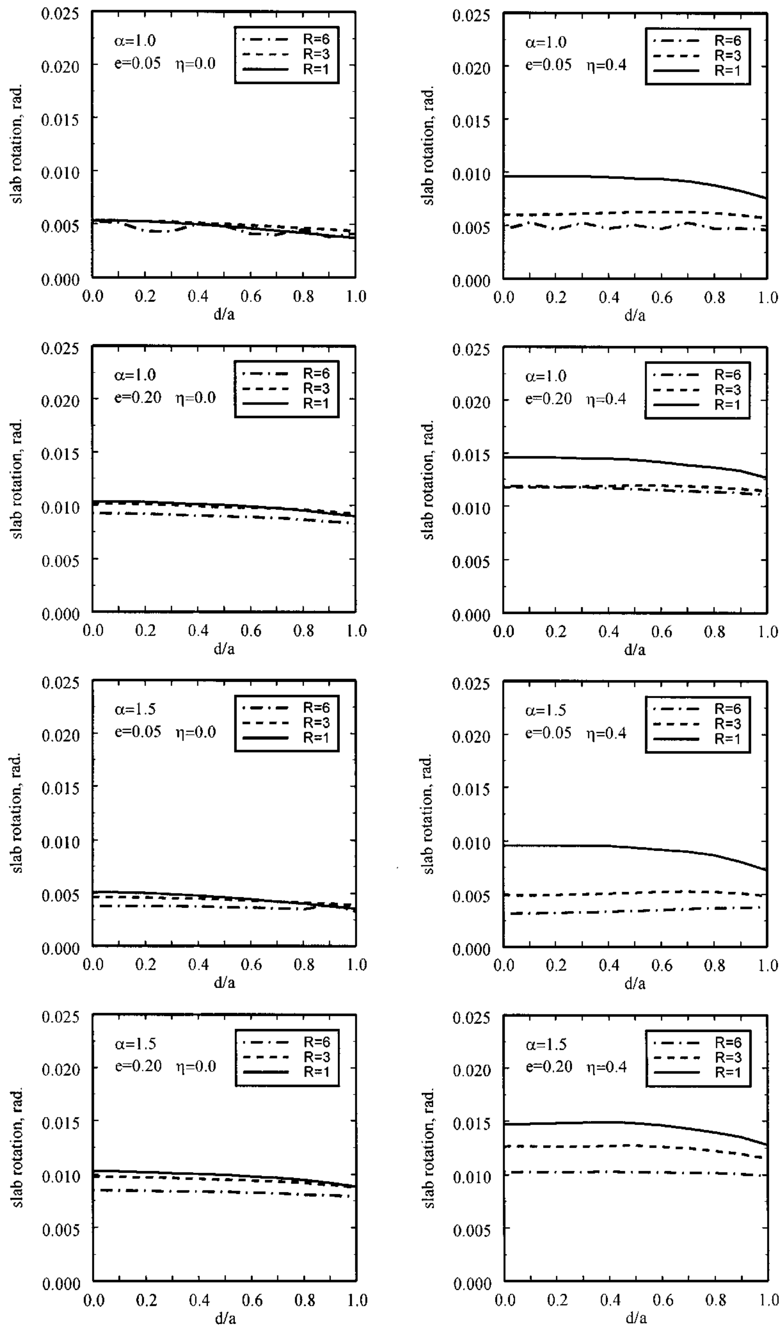

Figure 7. Slab rotation computed for systems with $\delta = 0{\cdot}0$ and $T = 0{\cdot}5$ s

in the second one. As expected from the values of ρ_k in Table I, however, rotations are larger for $\eta = 0{\cdot}4$ than for $\eta = 0{\cdot}0$.

Effect of the design factor α

The effect of factor α can be studied by analyzing the same Figures 6 and 7. As indicated before, each group consisting of the four upper graphs in these figures corresponds to systems designed with $\alpha = 1{\cdot}0$ and the group consisting of the four lower graphs corresponds to systems designed with $\alpha = 1{\cdot}5$. Thus, the effect of α can be assessed by comparing between corresponding graphs of these groups. As expected, results in Figure 6, which shows the normalized ductility demands of both resisting elements, indicate that ductility demand of element 1 (μ_{n1}) is not appreciably influenced by α. On the other hand, flexible-element graphs in the same Figure 6 show that μ_{n3} is smaller for systems designed with $\alpha = 1{\cdot}5$ than for systems designed with $\alpha = 1{\cdot}0$. Moreover, flexible elements of systems having small eccentricity ($e = 0{\cdot}05$) suffer a larger normalized ductility demand than corresponding elements of systems with large eccentricity ($e = 0{\cdot}20$). The same conclusions are obtained from results (not shown here) corresponding to systems with $\eta = 0{\cdot}0$. The reduction of μ_{n3} with e, which has been observed by other researchers,[3] suggests that smaller values of α can be used in systems with large stiffness eccentricity than in systems with small eccentricity.

Left-side graphs in Figure 7 show that slab rotation θ is not significantly influenced by α in systems without initial geometric eccentricity ($\eta = 0{\cdot}0$), independently of the value of R. Graphs on the right side, corresponding to $\eta = 0{\cdot}4$, indicate that slab rotation slightly decreases with α but only for large values of R.

Effect of the design factor δ

Factor δ has a significant effect on the rigid element. Figure 8 shows the computed normalized ductility demand of element 1 in terms of the ratio d/a for systems with $\eta = 0{\cdot}0$ (left-side graphs) and $\eta = 0{\cdot}4$ (right-side graphs). For all cases in this figure $\alpha = 1{\cdot}0$ and $T = 0{\cdot}5$s. The upper four graphs correspond to systems designed with $R = 1$ and the lower four graphs to systems designed with $R = 6$. Results are shown for three values of δ (0·0, 0·5, and 1·0) and for two values of the stiffness eccentricity: $e = 0{\cdot}05$ in first and third rows and $e = 0{\cdot}20$ in second and fourth rows. As expected, μ_{n1} grows with the increment of torsion-induced force reduction (value of δ). It can be observed that the value of $\delta = 0{\cdot}0$, which corresponds to neglect the negative shear forces induced by torsion, leads to ductility demands that do not exceed the values of corresponding elements of TB systems, i.e. $\mu_{n1} \leq 1{\cdot}0$. This agrees with the conclusion obtained by Wong and Tso[7] using *fully bidirectional* analyses. The same figure shows that for $e = 0{\cdot}20$, the effect of δ is more significant for $\eta = 0{\cdot}0$ than for $\eta = 0{\cdot}4$. This behaviour can be explained with aid of the lever-arm distances from the stiff- and flexible-side elements to the center of stiffness. For $\eta = 0{\cdot}0$ the initial distances of both elements to CR are equal, implying that the contribution of these elements to the torsional resistance is about the same. For $\eta = 0{\cdot}4$ (or $\eta = 0{\cdot}2$), the distance from the stiff element to CR is smaller than the distance corresponding to $\eta = 0{\cdot}0$. Thus, for $\eta = 0{\cdot}2$ and $\eta = 0{\cdot}4$ the torsional response is much governed by the flexible element than by the stiff one. Therefore, the effect of δ, which affects directly the stiff element is minimized. This is more noticeable for $e = 0{\cdot}20$ than for $e = 0{\cdot}05$.

For $\eta = 0{\cdot}0$, the value of $\delta = 0{\cdot}5$ conduces to normalized ductility demands slightly larger than 1·0 for systems with large eccentricity ($e = 0{\cdot}20$) only. For $\delta = 1{\cdot}0$ and $\eta = 0{\cdot}0$, values of μ_{n1} can be

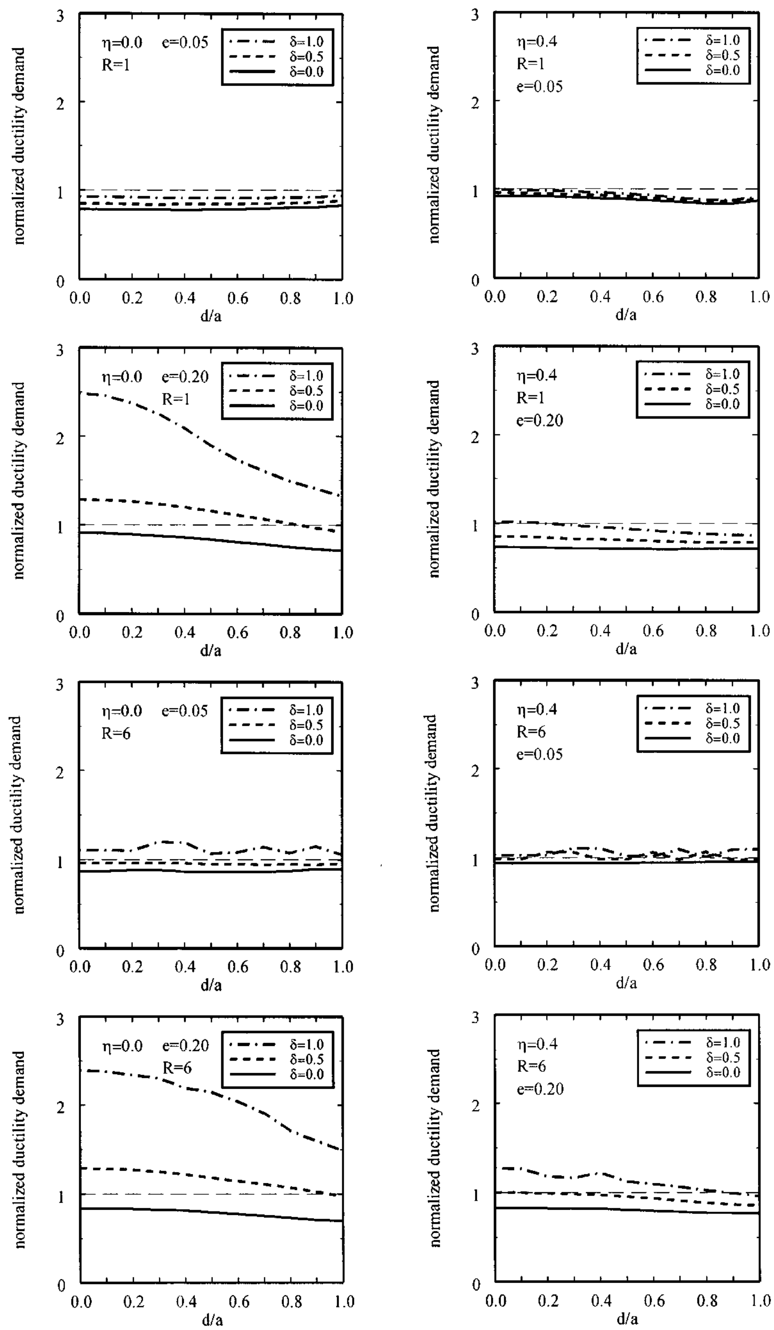

Figure 8. Normalized ductility demand of element 1 for systems with $T = 0{\cdot}5$ s and $\alpha = 1{\cdot}0$

significantly larger than 1·0. Left-side graphs indicate that the value of μ_{n1} is larger for $e = 0{\cdot}20$ than for $e = 0{\cdot}05$, which suggests that the value of $\delta = 0{\cdot}5$ would be acceptable for systems with small eccentricities. For large eccentricities, $\delta = 0{\cdot}5$ would be acceptable for systems with a small distance between CR and the stiff element. At this point it is interesting to recall that Zhu and Tso[17] recommend to use $\delta = 0{\cdot}5$.

Effect of the initial lateral (uncoupled) period T

Graphs in Figure 9 can be used to study the effect of the lateral period T. In these graphs the normalized ductility demands of elements 1 (left-side graphs) and 3 (right-side graphs) are plotted in terms of the ratio d/a for systems with $\eta = 0{\cdot}4$ and designed with $\alpha = 1{\cdot}0$ and $\delta = 0{\cdot}0$. Again, the four upper graphs correspond to $R = 1$ and the lower ones to $R = 6$. Results indicate that for the stiff element, μ_{n1} slightly increases with growing values of T. For the flexible element, μ_{n3} slightly decreases with increasing values of T. Thus, as noticed in Reference 3, estimates of displacement ductility demand of element 1 based on short-period systems can be (slightly) unconservative for systems with larger periods. Results indicate that the small effect of T seems to be independent of the magnitude of R and e.

Effect of the stiffness eccentricity e

The effect of e can be analysed with Figures 6–9 by comparing the first and third rows of each figure (corresponding to $e = 0{\cdot}05$) with the second and fourth rows (corresponding to $e = 0{\cdot}20$). Left-side graphs in Figure 6 indicate that μ_{n1} slightly reduces with growing values of e (see also left-side graphs in Figure 5). Right-side graphs in the same figure suggest that α can be specified in terms of e. The larger the stiffness eccentricity the smaller μ_{n3}. As a simple design recommendation, two values of α can be specified depending on the value of e: $\alpha = 1{\cdot}0$ for systems with large eccentricity ($e = 0{\cdot}20$) and $\alpha = 1{\cdot}5$ for systems with small eccentricity ($e \leq 0{\cdot}05$). A linear interpolation between these two values of α could be recommended for intermediate values of e. As expected, results in Figure 7 indicate that slab rotation increases with the stiffness eccentricity. Results in Figure 8 indicate that both eccentricities (e and η) are related to δ, as explained before. It can be observed in left-side graphs (corresponding to $\eta = 0{\cdot}0$) that the effect of e is small for systems designed with $\delta = 0{\cdot}0$ but it is large for systems designed with $\delta = 1{\cdot}0$. Finally, Figure 9 indicates that, for systems designed with $\delta = 0{\cdot}0$, the effect of e is about the same for all systems, independently of the the values of both the initial lateral period and the force reduction factor.

Effect of the distance between transverse elements d/a

All plots in Figures 6–9 are presented in terms of the normalized distance between *transverse* elements d/a (elements 4 and 6 in Figure 1). As noticed before, the value of $d/a = 0{\cdot}0$ corresponds to the case where these elements are uncoupled of the system torsional response while the value of $d/a = 1{\cdot}0$ corresponds to the largest system torsional stiffness. It can be observed in the left-side graphs of Figure 6 that μ_{n1} does not vary significantly with d/a for $\delta = 0{\cdot}0$. On the other hand, the value of μ_{n3} (right-side graphs) increases with growing values of d/a. These results are consistent with the observation made by Correnza *et al.*[8] related to the difference between uni- and bi-directional analyses in flexible elements of short-period systems. It is interesting to note that

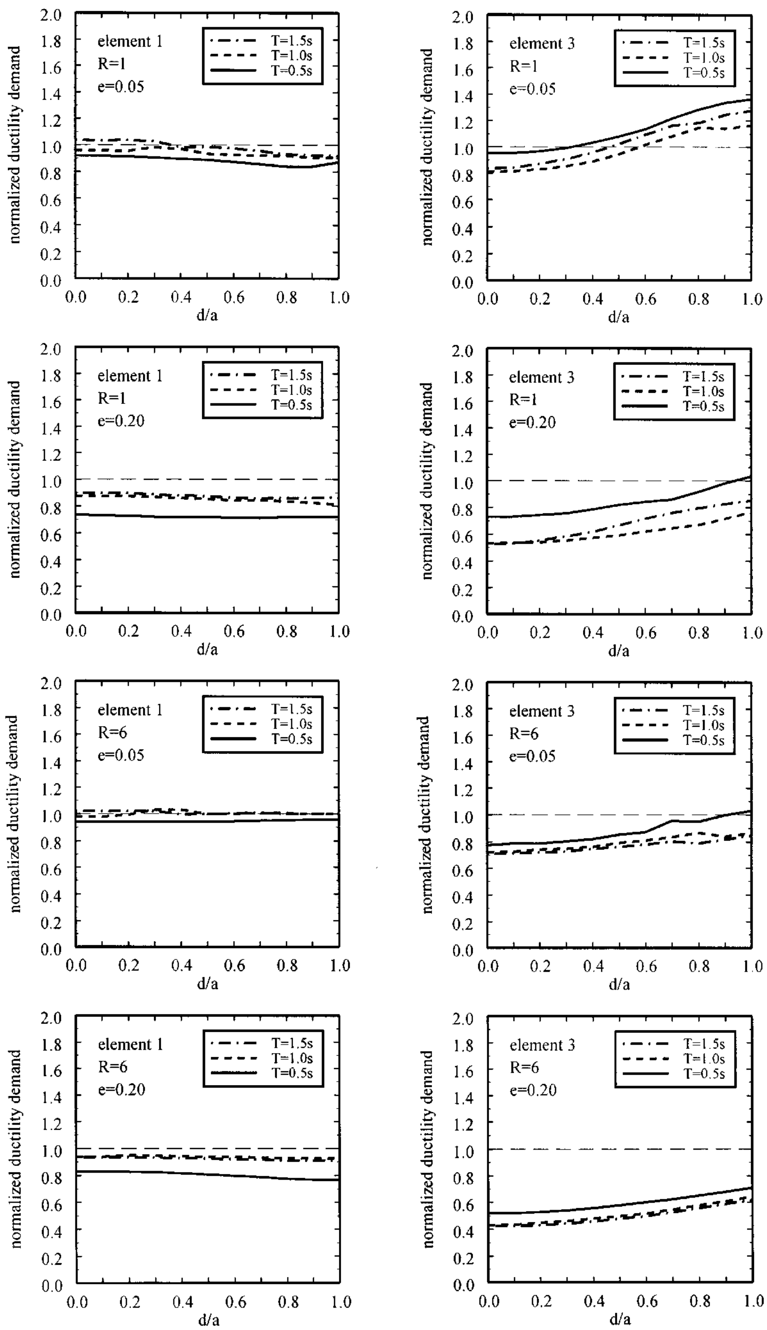

Figure 9. Normalized ductility demands of elements 1 and 3 for $\eta = 0{\cdot}4$, $\alpha = 1{\cdot}0$ and $\delta = 0{\cdot}0$

even though increasing values of d/a lead to growing values of system torsional stiffness and strength, μ_{n3} grows appreciably in Figure 6. This behaviour can be explained as follows. When d/a increases, the participation of transverse elements increases, reducing the design force of element 3. The design force of element 1 does not vary significantly in this case ($\delta = 0{\cdot}0$). Because strength reduction of element 3 is larger than the total system strength increment caused by the d/a variation, the net result is an increment of μ_{n3}. The magnitudes of both the strength reduction of element 3 and the system overstrength (for several building codes) is documented by Chandler and Duan.[3]

In Figure 8 (corresponding to systems with $T = 0{\cdot}5$ s and designed with $\alpha = 1{\cdot}0$) the curves for $\eta = 0{\cdot}0$, $\delta = 1{\cdot}0$, and $e = 0{\cdot}20$ show that μ_{n1} decreases significantly with growing values of d/a. This case exemplifies another difference between uni- and bi-directional analyses which was not anticipated by Correnza *et al.*[8] Moreover left-side graphs of Figure 9 suggest that similar trends could apply to systems with longer periods. The reduction of μ_{n1}, shown in Figure 8, is due to the allowance of strength reduction of element 1 when $\delta = 1{\cdot}0$ is used.

CONCLUSIONS

In this paper, the effect of several design factors on the seismic response of torsionally unbalanced systems was studied using nonlinear fully-bidirectional analyses and an ensemble of ten earthquake records. The main conclusions obtained from this study are the following.

1. Computed normalized ductility demands of the flexible resisting element μ_{n3} indicate that, in order to attain values of μ_{n3} close to 1·0, the design factor α should depend on the seismic-force reduction factor R, the initial lateral period T, and the initial stiffness eccentricity e. Results indicate that α should be increased with: (i) decreasing values of R, (ii) decreasing values of T, and (iii) decreasing values of e.
2. Computed slab rotations θ are reduced with increasing values of the force reduction factor R. However, they are not significantly affected by the selected value of both α and d/a. Due to differences of torsional stiffnesses, slab rotation was found to be larger for systems with $\eta = 0{\cdot}4$ than for systems with $\eta = 0{\cdot}0$.
3. Computed normalized ductility demands of the stiff resisting element μ_{n1} indicate that, in order to attain values of μ_{n1} close to 1·0, the design factor δ should depend on: the initial lateral period T, the geometrical eccentricity η, and the initial stiffness eccentricity e. It was found that the μ_{n1} is not significantly influenced by R. Results indicate that the value of $\delta = 0{\cdot}0$ maintains the value of the ductility demand of the rigid resisting element in TU systems below the corresponding demand in TB systems. It was found that a value of $\delta = 0{\cdot}5$ can be acceptable for the following cases: (i) systems with small stiffness eccentricity e and (ii) systems with large stiffness eccentricity e and large value of geometrical eccentricity η.
4. The effect of the lateral period T on the normalized ductility demand of both the stiff and the flexible side elements was found to be small. The following trends were found with increasing values of the lateral period T: the normalized ductility demand of the stiff element increases and that of the flexible element decreases.
5. Increasing values of the stiffness eccentricity e lead to: (i) decreasing values of the normalized ductility demands μ_{n1} and μ_{n3}, (ii) increasing hysteretic work of the flexible element, and (iii) decreasing hysteretic work of the stiff element.

6. Observed differences between results obtained by using unidirectional analyses and fully-bidirectional analyses suggest that additional study should be carried out to assess the equivalence between these two types of analysis to study torsion-related problems.

REFERENCES

1. R. K. Goel and A. K. Chopra, 'Inelastic seismic response of one-story, asymmetric-plan systems', *EERC Report No. 90/14*, Earthquake Engineering Research Center, University of California at Berkeley, CA, 1990.
2. W. K. Tso and T. J. Zhu, 'Design of torsionally unbalanced structural systems based on code provisions, I: ductility demand', *Earthquake Engng. Struct. Dyn.* **21**, 609–627 (1992).
3. A. M. Chandler and X. N. Duan, 'Performance of asymmetric code-designed buildings for serviceability and ultimate limit states', *Earthquake Engng. Struct. Dyn.* **26**, 717–735 (1997).
4. Associate Committee on the Nation Building Code, *National Building Code of Canada*, National Research Council of Canada, Ottawa, Ontario, 1995.
5. Departamento del Distrito Federal, *Reglamento de Construcciones para el Distrito Federal*, México, D.F., 1993.
6. *International Conference of Building Officials*, *Uniform Building Code*, Whittier, CA, 1991.
7. C. M. Wong and W. K. Tso, 'Evaluation of seismic torsional provisions in Uniform Building Code', *J. Struct. Engng. ASCE* **121**, 1436–1442 (1995).
8. J. C. Correnza, G. L. Hutchinson and A. M. Chandler, 'Effect of transverse load-resisting elements on inelastic-earthquake response of asymmetrical-plan buildings', *Earthquake Engng. Struct. Dyn.* **23**, 75–89 (1994).
9. R. K. Goel, 'Seismic response of asymmetric systems: energy based approach', *J. Struct. Engng. ASCE* **123**, 1444–1453 (1997).
10. M. De Stefano, G. Faella and R. Ramasco, 'Inelastic seismic response of one-way plan-asymmetric systems under bidirectional ground motions', *Earthquake Engng. Struct. Dyn.* **27**, 363–376 (1998).
11. R. Clough and S. Johnston, 'Effect of stiffness degradation on earthquake ductility requirements', *Japan Earthquake Engineering Symp.*, Tokyo, 1966, pp. 195–198.
12. S. Otani, 'Hysteresis models of reinforced concrete for earthquake response analysis', *J. Faculty Engng. B* (*University of Tokyo*) **36**(2), 125–159 (1981).
13. R. Riddell and N. M. Newmark, 'Statistical analysis of the response of nonlinear systems subjected to earthquakes', *Struct. Research Series No. 468*, Department of Civil Engineering, University of Illinois at Urbana-Champaign, IL, 1979.
14. N. M. Newmark and W. J. Hall, *Earthquake Spectra and Design*, Earthquake Eng. Res. Inst., Berkeley, CA, 1982.
15. T. Paulay, Displacement-based design approach to earthquake-induced torsion in ductile buildings', *Engng. Struct.* **19**, 699–707 (1997).
16. T. Paulay, 'Torsional mechanisms in ductile building systems', *Earthquake Engng. Struct. Dyn.* **27**, 1101–1121 (1998).
17. T. J. Zhu and W. K. Tso, 'Design of torsionally unbalanced structural systems based on code provisions, II: strength distribution', *Earthquake Engng. Struct. Dyn.* **21**, 629–644 (1992).

